J Sol-Gel Sci Technol (2011) 58:6–11
DOI 10.1007/s10971-010-2347-x

ORIGINAL PAPER

Preparation and characterization of diphasic sol-gel derived unsupported mullite membranes

Berna Topuz · Muhsin Çiftçioğlu

Received: 14 July 2010 / Accepted: 14 October 2010 / Published online: 26 October 2010

Abstract Diphasic gels prepared by mixing freshly prepared polymeric silica and polymeric boehmite sols through a modified Al-alkoxide route in mullite compositions led to the crystallization of mullite upon heat treatment at 775 °C. Mullite formation was observed at a 100 °C higher temperature when diphasic gels were formed by mixing aged polymeric sols containing about 2 nm in diameter boehmite species. These relatively low mullite formation temperatures were attributed to the nanoscale sizes of the polymeric species of the two amorphous phases present in the diphasic gels.

Keywords Diphasic gel · Mullite crystallization · Sol-gel · Unsupported ceramic membrane

1 Introduction

Mullite ($3Al_2O_3{\cdot}2SiO_2$) is a very important ceramic phase due to its thermal, mechanical and optical properties like low thermal expansion ($4.5 \times 10^{-6}{}^{\circ}C^{-1}$), low thermal conductivity (6 kcal $m^{-1}h^{-1}$ $^{\circ}C^{-1}$ at 20 °C), and good chemical and oxidation resistance [1]. It is the only stable binary phase in contact with a liquid at high temperatures in the Al_2O_3–SiO_2 system [2]. It is assumed that stable mullites exist in the range of compositions between $3Al_2O_3{\cdot}2SiO_2$ (3:2) and $2Al_2O_3{\cdot}SiO_2$ (2:1) [3]. Sol-gel processing has been used during the last decade for mullite preparation with chemically homogeneous microstructures [4–9]. The observation of mullitization at relatively low temperatures is commonly reported to be due to molecular-nano scale mixing of the precursor phases achieved through sol-gel processing. However, differences in hydrolysis rates of Al^{3+} and Si^{4+} alkoxides may create significant segregation tendencies thus preventing the formation of a chemically homogeneous mullite forming precursor on a nanoscale/molecular level. A variety of synthetic precursors for the crystallization of mullite phase with high chemical purity, high sinterability and mullite formation temperatures below 1,250 °C through solid state reactions have been reported [10].

Mullite precursors can be classified as either single phase (atomic level homogeneity) or diphasic (homogeneity in nanometer–micrometer range). Single phase precursors obtained by using chemical vapour deposition, spray pyrolysis and polymer based methods exhibit direct mullitization from the amorphous state at temperatures as low as 950 °C, while diphasic precursors mullitize above 1,200 °C by the reaction of transient spinel alumina with silica. The behaviour of a mullite precursor is a direct result of the starting materials and of the synthesis conditions [11, 12]. In single phase mullite formation, due to the atomic-scale arrangement of –Al–O–Si– bond in amorphous phase precursor, the crystallization of mullite occurs by a nucleation controlled process. The reaction between alumina surfaces and amorphous silica matrix causes the formation of mullite at temperatures in the 1,200–1,350 °C range and can be expressed as following for the diphasic system [13];

$$3(\delta - Al_2O_3) + 2(\text{amorphous } SiO_2) \rightarrow 3\ Al_2O_3 \cdot 2 \cdot SiO_2(\text{mullite}) \quad (1)$$

The mullite formation kinetics for the diphasic systems have been determined as the nucleation and growth process

B. Topuz (✉) · M. Çiftçioğlu
Chemical Engineering Department, İzmir Institute of Technology, Urla, İzmir 35430, Turkey
e-mail: bernatopuz@gmail.com

M. Çiftçioğlu
e-mail: muhsinciftcioglu@iyte.edu.tr

in which the controlling step is the diffusion of reactants to the growth interface and the rate of mullite formation is much slower than that in single phase system [14]. Sunderesan and Aksay, [13] stated that after low-temperature (<1,350) nucleation of mullite within the matrix, growth is controlled by the dissolution of alumina in the amorphous silica matrix but not by interdiffusion through the mullite phase.

The development of mullite membranes with microporous networks would have particular importance due to its high thermal stability. Microporous membrane structure has been reported for the 450 °C heat treated alumina-silica membranes derived from mixed TEOS and urea stabilized alumina hydrosol in the study of Cheraitia et al. [15].

The research results on improving the stability of sol-gel derived silica and alumina based membranes and the resultant gas permeation behaviour were reported previously [16–18]. The prepared meso/microporous alumina and silica gas separation membranes formed the thin selective top layer on disc shaped macroporous alumina supports (40 mm in diameter and 2 mm in thickness). In this study, sol-gel derived unsupported alumina-silica membranes were prepared by mixing stable polymeric boehmite and silica sols in mullite composition (Al:Si molar ratio of 3:1). The use of polymeric boehmite sols prepared through controlled hydrolysis of modified aluminium-alkoxide with low water to alkoxide ratios made the preparation of stable diphasic boehmite-silica sols possible. Mullite crystallization temperatures in these diphasic polymeric gels were further determined. The pore and phase structure characterizations on the selective thin layers on various macroporous supports can only be conducted on their unsupported counterparts in ceramic membrane research.

2 Materials and methods

The unsupported membrane preparation procedure is schematically given in Fig. 1. Polymeric boehmite sols with water contents lower than theoretically required for complete hydrolysis and condensation reactions were prepared by controlling the rate of these reactions [18]. Ethyl-acetoacetate (EAA; 99%-Fluka) was used as chelating agent to modify the Aluminum-trisecbutoxide (ASB; 97%-Merck) in order to prepare stable sols. The hydrolysis/condensation reactions of EAA modified precursor was conducted at 90 °C for 3 h after the drop-wise addition of predetermined H_2O and HNO_3-ASB/2-Butanol/EAA mixture with constant vigorous stirring. The sol molar ASB:2-Butanol:EAA:HNO_3:H_2O ratio was 1:18:0.1:0.35:2. The polymeric silica sol was also prepared by acid catalysed hydrolysis and condensation of tetraethylorthosilicate (TEOS; 98%-Aldrich) in ethanol (99.8%-Riedel). Predetermined water and nitric acid solutions were added drop-wise to the TEOS/ethanol mixture placed in an ice bath to prevent partial hydrolysis [19]. After the addition was completed, the reaction mixture was heated to 60 °C for 3 h under constant stirring in a glove box. The standard silica sol molar TEOS:HNO_3:H_2O:EtOH ratio was 1:0.085:6.4:3.8.

The stable polymeric boehmite sol was mixed with polymeric silica sol in Al_2O_3:SiO_2 mole ratio of 3:2. 60 °C

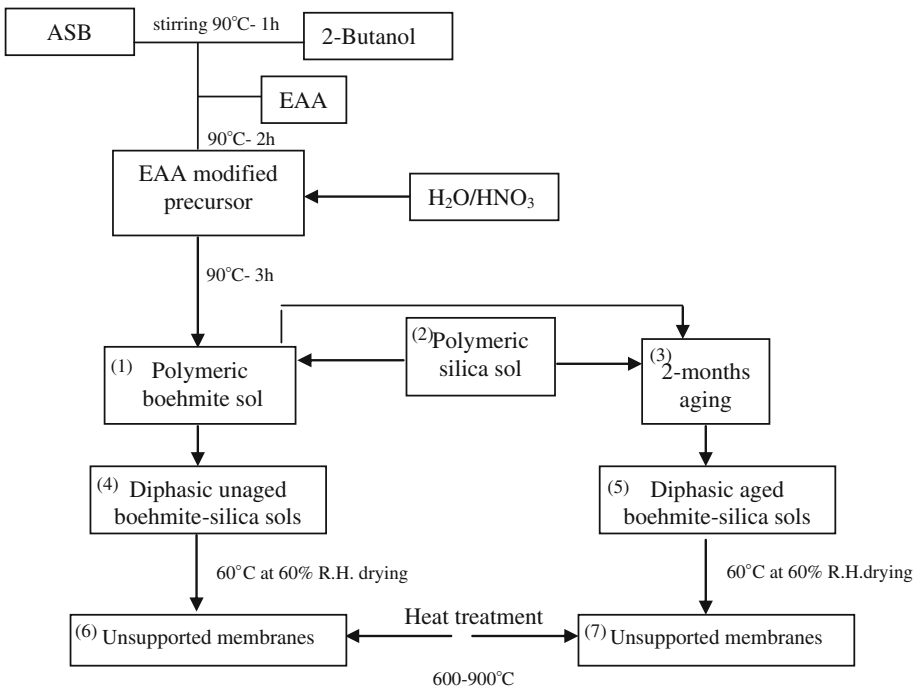

Fig. 1 Flowchart of unsupported diphasic mullite membrane preparation with labelled important processing step number (#)

overnight dried at a relative humidity (R.H.) of 60% (Binder-KBF 115, Constant Climate Chamber) unsupported membranes were heat treated in the 600–900 °C range for 1 h with a heating rate of 5 °C/min (Carbolite-CWF 1300).

2.1 Membrane characterization

Dynamic light scattering (DLS) was used to determine the particle size distribution in the diluted sols at 25 °C (ZetaSizer 3000 HS, Malvern). The particle size distribution obtained from DLS measurements is based on intensity of light scattered and it is possible to convert size distributions into volume/number based distributions by using Mie theory [20]. Although, there is a direct relation between the diameter (D) and the number, volume fraction is proportional to D^3. In general, measured particle sizes are in the order of intensity > volume > number. FTIR spectroscopy (FTIR-8400S, Schimadzu Co.) was carried out to determine the molecular functional groups while X-ray diffraction (Philips X'pert Pro) with CuK_α was employed for phase structure characterization within the 2θ range of 5–80°. TGA (TGA-51/51H, Shimadzu) was used for thermal characterization where the samples were heated at a rate of 10 °C/min up to 1,000 °C. The densification behaviour of unsupported membrane powders were investigated by determining the dilatometric shrinkage curves (Linseis, L76/150B) with a heating rate of 5 °C/min up to 1,300 °C. The 60 °C dried unsupported membranes were consolidated by uniaxial pressing under a pressure of 180 MPa for dilatometric runs.

3 Results and discussions

DLS derived particle size distributions of boehmite sols aged in a refrigerator (+4°C) for 2 months are given in Fig. 2. Although number based average particle size was

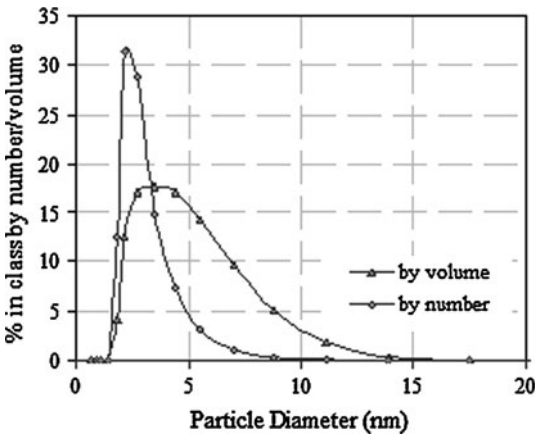

Fig. 2 DLS particle size distributions of 2 months aged (processing step #3 sols) polymeric boehmite sol

2.2 nm, a wider volume based particle size distribution with a peak at about 3.5 nm was obtained. It was not possible to determine the particle size distributions of freshly prepared polymeric boehmite and silica sols by dynamic light scattering. The determination of the sizes of the particles in the 1–2 nm (the lower range of the DLS equipment) range with the Zetasizer is possible in sols according to our extensive experience on various sol characterizations. It is most likely that species with sizes lower than 1 nm was present in the freshly prepared boehmite/silica sols and aged silica sols prepared in this work.

Mullite has both AlO_4 tetrahedra and AlO_6 octahedra connected to SiO_4 and in FTIR spectra the characteristic peaks of Al–O and Si–O bonds are in the 1,200–400 cm^{-1} range [21]. The characteristic standard mullite phase bands are the following: tetrahedral (SiO_4) (Si–O) vibrations at 1,130 and 1,170 cm^{-1}, tetrahedral (AlO_4) (Al–O) vibrations at 730 and 820 cm^{-1}, and octahedral (AlO_6) (Al–O) vibrations in the range of 530–680 cm^{-1}. The two bands for AlO_4 and AlO_6 probably each result from Si–O–Al and Al–O–Al bonds [12, 22]. The FTIR spectra of alumina-silica unsupported membranes as a function of heat treatment are given in Fig. 3. FTIR band at 1,170 cm^{-1} is more intense than the band at 1,130 cm^{-1} for orthorhombic mullite, while the opposite indicates the domination by the tetragonal phase [23]. The absence of band in the 1,070–1,090 cm^{-1} range indicates that there is no amorphous silica phase in the oxide network [8]. Broad peak observed at 1,100 cm^{-1} for temperatures of 600 and 800 °C shifted upon heat treatment above 850 °C and the spectra show a strong band at ~1,110 cm^{-1}, with a weak shoulder which is attributed to tetrahedral (Si–O) vibrations in mullite. For all heat treated samples, band located that 670 cm^{-1} and broad envelope centered at about 815 cm^{-1} most likely results from mixed bands due to AlO_4 and AlO_6 (Al–O) vibrations in mullite. The bands at 570 and 620 cm^{-1} for all samples are due to octahedral (AlO_6) (Al–O) vibrations.

The mixture of aged polymeric silica and polymeric boehmite sols in mullite compositions (3:2) led to the crystallization of mullite upon heat treatment at 875 °C as evidenced by peaks at 2θ values of ~16, 26, and 35° etc. These peaks correspond to the stoichiometric mullite, $3Al_2O_3{\cdot}2SiO_2$ (JCPDS, file 15–776). The crystallite sizes of 900 °C heat treated mullite unsupported membranes are in the 20–40 nm range as tabulated in Table 1. XRD patterns of diphasic alumina and silica and pure polymeric silica unsupported membranes are shown in Fig. 4. There is no indication for the formation of the spinel phase (sharp 2θ peaks at 46 and 67°) indicating the formation of a very homogeneous structure because of a high degree of mixing [12, 23]. A transient phase (spinel) formation is generally

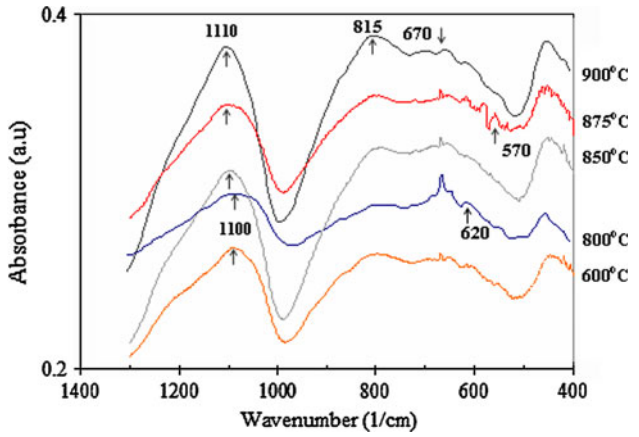

Fig. 3 FTIR spectra of unsupported diphasic alumina-silica membranes (processing step #6 dried and heat treated materials) heat treated at different temperatures

Table 1 XRD crystallite sizes of aged sols derived mullite membranes (processing step #7 dried and heat treated materials) heat treated at 900 °C

Phase	°2θ	D_{hkl} (nm)	°2θ	D_{hkl}(nm)
$3Al_2O_3{\cdot}2SiO_2$	16.55	30	42.7	20
	26.25	23	47.5	23
	31.10	41	53.8	25
	33.30	25	60.7	28
	39.40	37	64.7	25

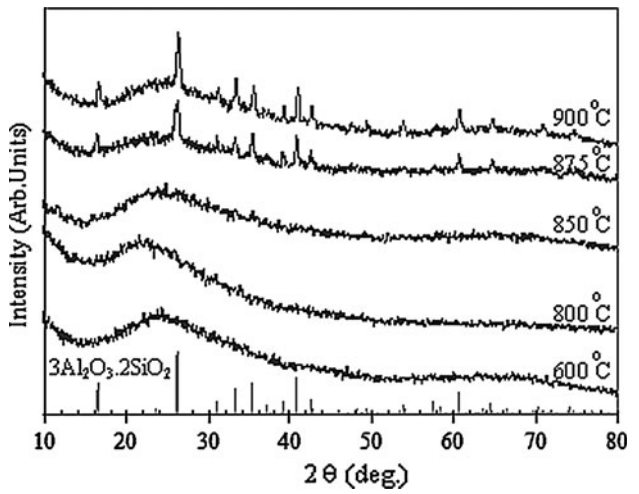

Fig. 4 XRD patterns of unsupported mullite membranes derived from aged sols (processing step #7 dried and heat treated materials)

observed in the diphasic systems due to heterogeneities created by uncontrolled hydrolysis reactions before mullite crystallization [23].

XRD patterns of pure polymeric alumina and silica unsupported membranes heat treated in the 600–800 °C range are given in Figs. 5 and 6. Three γ-Al_2O_3 peaks (gamma phase: JCPDS, card file 10–0425) were identified in the 800 °C heat treated membrane pattern while heat treatment below 800 °C resulted in fully amorphous structures. It is also evident from the same XRD pattern that although the dominant phase was gamma, alpha phase crystallization (alpha phase: JCPDS, card file 46–1,212) had also started at 800 °C.

XRD patterns indicate that the diphasic precursor material is completely amorphous until at least 875 °C while the silica and boehmite polymeric gels show distinctive cristobalite and gamma–alpha alumina crystallization at 800 °C as shown in Figs. 5 and 6. The absence of these peaks in the diphasic heat treated gels is a strong indication of homogeneous mixing and the formation of a very fine and stable amorphous microstructure.

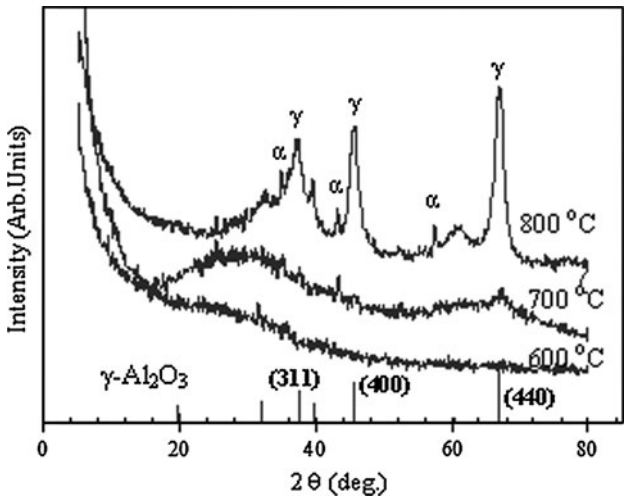

Fig. 5 XRD patterns of unsupported alumina membranes treated at various temperatures (JCPDS, file 10-0425) [18]

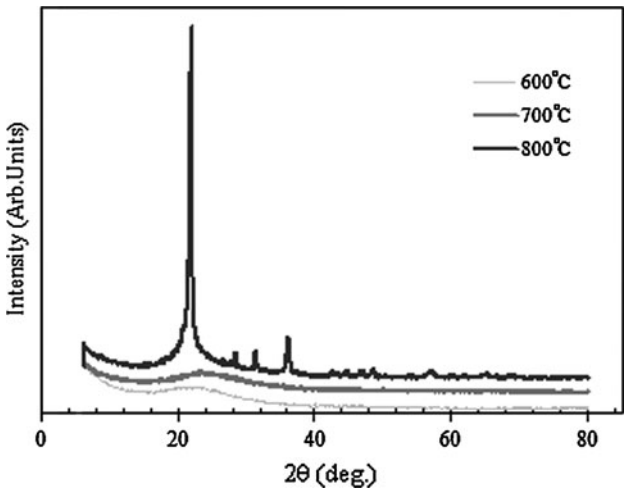

Fig. 6 XRD patterns of unsupported silica membranes treated at various temperatures (cristobalite phase: JCPDS, file 76-0941)

The corresponding dilatometric shrinkage and shrinkage rate curves of unsupported mullite membrane powder pellet prepared from aged sols are given in Fig. 7. Rapid shrinkage at 150 °C may be due to the removal of solvent ($B{\cdot}P{\cdot}_{Butanol} = 99$ °C). At temperatures below 400 °C shrinkage of sample could be due to the removal of organics and polymerization and rearrangement of the diphasic structure. The weight loss above 400 °C was negligible as observed from the TGA curve (Fig. 7a). A second shrinkage event starts at about 875 °C which is the mullite crystallization temperature determined from the XRD patterns of membranes prepared from aged sols where the shrinkage rate is highest at 945 °C. It is thus likely that shrinkage due to the nucleation and growth of mullite crystals occurs in the 875–1,000 °C range. Two smaller mullite crystallization/densification peaks appear at 1,120 and 1,220 °C in the densification rate curve. These are the temperatures which are commonly reported as mullite crystallization temperatures in the diphasic gels. The final linear shrinkage was about 40%.

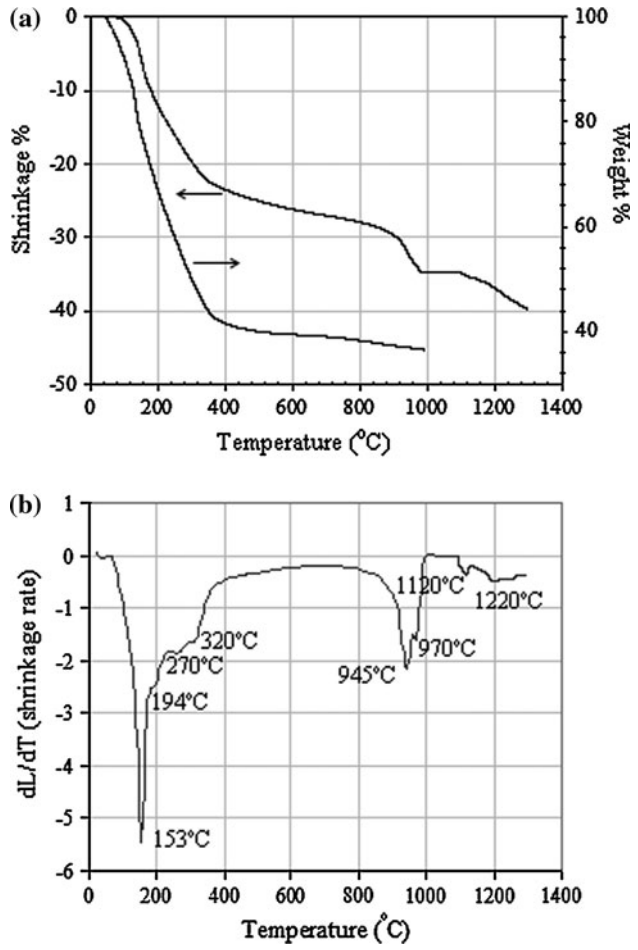

Fig. 7 **a** Shrinkage and TGA **b** shrinkage rate curves for diphasic alumina-silica gels (processing step #7 dried materials) derived from aged sols

The use of freshly prepared sols for mullite formation decreased the crystallization temperature as shown in Fig. 8 due to the presence of smaller particles in unaged sols. The transformation to crystalline mullite from the amorphous matrix starts to occur at 775 °C and the mullite peaks became sharper at 800–850 °C due to nucleation/grain growth. Besides the presence of about 1–2 nm polymeric boehmite species, the low transformation temperature could also be attributed to the highly reactive amorphous silica derived from polymeric sol-gel route. The degree of chemical homogeneity has a significant role for determining the mullite formation mechanism and thus mullite crystallization temperature. Vol'khin et al. [24] stated that decreasing the particle size of the mullite precursors decreases the mullitization temperature. Kansal et al. [12] used the splitting of the peak at 26.15° 2θ in tetragonal mullite (on heat treatment at temperatures above 1,000 °C) as a means of estimating the extent of conversion of the tetragonal phase to the orthorhombic phase. Orthorhombic phase is a more stable structure compared to the metastable tetragonal phase which is characterized by the XRD peak at 26.15° (2θ CuKα) [23]. The extended scale of 2θ values in 25–27° range is shown in the insert in Fig. 8. Splitting of (120) and (210) peaks was observed in the 775 and 800 °C patterns which is commonly accepted as a direct indication of orthorhombic mullite formation. Splitting of peaks on the other hand was not observed in the 850 °C pattern.

The presence of sharp mullite peaks above 775 °C in an amorphous matrix phase indicates the presence of significant level of mullite crystallinity and the variation of the XRD derived mullite crystallite sizes with temperature is given in Fig. 9. The small variation in crystallite size with heat treatment temperature indicated the stability of the

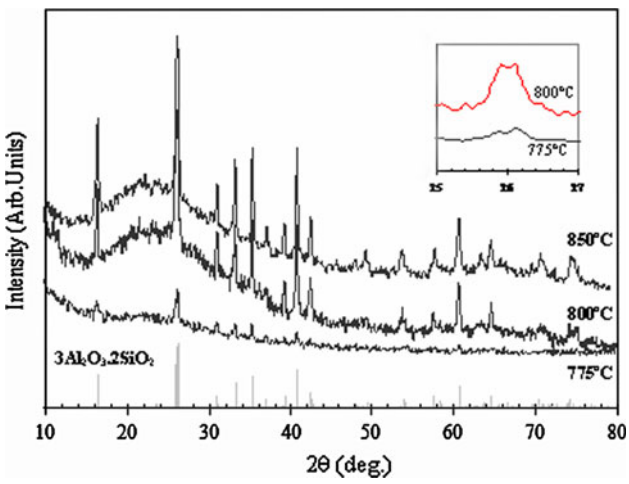

Fig. 8 XRD patterns of unsupported mullite membranes (processing step #6 dried and heat treated materials) prepared by using freshly prepared sols

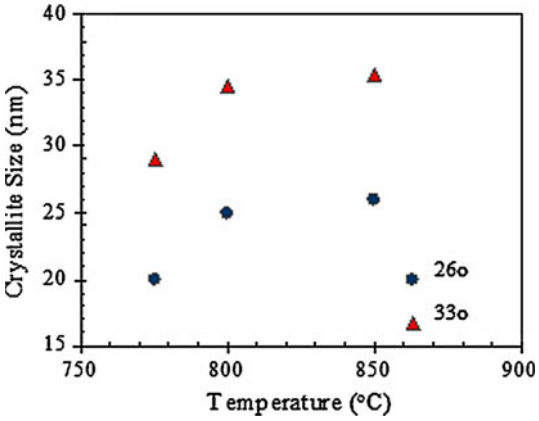

Fig. 9 Crystallite size variations of membranes (processing step #6 dried and heat treated materials) derived from freshly prepared sols

microstructure with insignificant coarsening in this temperature range. The XRD mullite crystallite sizes in the heat treated aged and unaged unsupported membranes are about in the same size range of 20–40 nm in the 775–900 °C range.

4 Conclusions

Diphasic alumina-silica sols/gels were prepared by using stable polymeric boehmite and silica sols. Low temperature mullitization in the 775–900 °C range was observed in the unsupported heat treated membranes due to the presence of homogeneous atomic/nanoscale mixing in the diphasic amorphous matrix. The mullitization temperature was determined to be about 100 °C higher when the polymeric boehmite sols were aged for 2 months causing formation of significantly larger alumina rich species and heterogeneities in the mixed amorphous matrix. Further study on the preparation of the supported mullite membranes may contribute significantly to a better understanding of the separation behaviour of these stable promising materials.

References

1. Schneider H, Schreuer J, Hildmann B (2008) J Eur Ceram Soc 28:329–344
2. Kleebe HJ, Siegelin F, Straubinger T, Ziegler G (2001) J Eur Ceram Soc 21:2521–2533
3. de Sola ER, Estevan F, Alarcon J (2007) J Eur Ceram Soc 27:2655–2663
4. Cassidy DJ, Woolfrey JL, Bartlett JR, Ben-Nissan B (1997) J Sol-Gel Sci Technol 10:19–30
5. Treadwell DR, Dabbs DM, Aksay IA (1996) Chem Mater 8(8):2056–2060
6. Marques Fonseca AML, Ferreira JMF, Miranda Salvado IM, Baptista JL (1997) J Sol-Gel Sci Technol 8(1–3):403–407
7. He F, Petuskey WT (2009) Mater Lett 63:2631–2634
8. Bagchi B, Das S, Bhattacharya A, Basu R, Nandy P (2009) J Am Ceram Soc 92(3):748–751
9. Osawa CC, Bertran CA (2005) J Braz Chem Soc 16(2):251–258
10. Griggio F, Bernardo E, Colombo P, Messing GL (2008) J Am Ceram Soc 91(8):2529–2533
11. Kojdecki MA, Ruiz de Sola E, Javier SF, Delgado-Pinar E, Mercedes RM, Javier EV, Maria Amigo J, Alarco'n J (2007) J Appl Cryst 40:260–276
12. Kansal P, Laine RA, Babonneau F (1997) J Am Ceram Soc 80(10):2597–2606
13. Sunderesan S, Aksay İA (1991) J Am Ceram Soc 74(10):2388–2392
14. Li DX, Thomson WJ (1990) J Am Ceram Soc 73(4):964–969
15. Cheraitia A, Ayral A, Julbe A, Rouessac V, Satha H (2010) J Porous Mater 17(3):259–263
16. B Topuz, Ph.D. Dissertation, İzmir Institute of Technology, İzmir, Turkey, 2009
17. Topuz B, Çiftçioğlu M (2010) J Membr Sci 350:42–52
18. Topuz B, Çiftçioğlu M (2010) J Sol-Gel Sci Technol doi: 10.1007/s10971-010-2305-7
19. de Vos RM, Verweij H (1998) J Membr Sci 143:37–51
20. Nobbmann U, Morfesis A (2009) Mater Today 12(5):52–54
21. Padmaja P, Warrier KGK, Padmanabhan M, Wunderlich W, Berry FJ, Mortimer M, Creamer NJ (2006) Mater Chem Phys 95:56–61
22. Orefice RL, Vasconselos WL (1997) J Sol-Gel Sci Technol 9:239–249
23. Cividanes LS, Campos TMB, Rodrigues LA, Brunelli DD, Thim GP (2010) J Sol-Gel Sci Technol 55:111–125
24. Vol'khin VV, Kazakova IL, Pongratz P, Halwax E (2000) Inorg Mater 36:375–379